

Does generation of magnetic storm depend on type of solar wind?

N. S. Nikolaeva,¹ Yu. I. Yermolaev,¹ I. G. Lodkina,¹

arXiv:1602.05826v1 [physics.space-ph] 18 Feb 2016

¹Space Plasma Physics Department,
Space Research Institute, Russian Academy
of Sciences, Profsoyuznaya 84/32, Moscow
117997, Russia. (nnikolae@iki.rssi.ru)

Abstract.

The purpose of this work is to draw attention of readers to a problem of possible differences in generation of magnetic storms induced by various large-scale solar wind (SW) streams: CIR, Sheath and ICME (including MC and Ejecta). Recently we showed that when using a modification of formula by *Burton et al.* [1975] for connection of interplanetary conditions with Dst and Dst^* indices the efficiency of storm generation by Sheath and CIR is $\sim 50\%$ higher than generation by ICME [*Nikolaeva et al.*, 2013, 2015]. In the literature there are many various functions coupling (FC) various interplanetary parameters with magnetospheric state. In this work we study the efficiency of main phase storm generation by different SW streams when using 12 another FCs on the basis of OMNI data during 1976–2000. Obtained results show that for most part of FCs Sheaths have the highest efficiency and MCs have the lowest efficiency in accordance with our previous results. The reliability of the obtained data and possible reasons of divergences for various FCs and various SW types require further researches.

1. Introduction

One of the unsolved problems of magnetosphere is its reaction on the solar wind (SW) variations. On the one hand, in the literature there are many functions coupling (FC) interplanetary conditions with magnetospheric state. The most of them are different functional forms of the solar wind electric field Ey , expressed through various parameters of the SW stream [Burton *et al.*, 1975; Kan and Lee, 1979; Hardy *et al.*, 1981; Holzer *et al.*, 1982; Wygant *et al.*, 1983; Newell *et al.*, 2007; Borovsky and Birn, 2014]. Another approach was used by Borovsky [2008, 2013a, b, 2014]: they estimated how local plasma parameters near the reconnection region (between magnetosheath and magnetosphere) control the reconnection on the dayside of the magnetosphere. He found the formula for local reconnection rate at the dayside of the magnetosphere R_{quick} by using the equation of Cassak and Shay [2007] for local reconnection rate between the two asymmetric plasmas near the magnetopause boundary. Additionally it was obtained the coupling function $FC = V_{sw} + 56Bs$, which does not have clear physical interpretation, but gives the more higher correlation with geomagnetic indices than any of electric field functions or reconnection functions [Borovsky, 2014]. These FCs are usually used for all available data during long intervals of measurements.

On the other hand, one of the recent experimental facts is that magnetic storms generated by different types of solar wind streams are different [Borovsky and Denton, 2006; Huttunen *et al.*, 2006; Pulkkinen *et al.*, 2007; Yermolaev *et al.*, 2007; Plotnikov and Barkova, 2007; Longden *et al.*, 2008; Turner *et al.*, 2009; Guo *et al.*, 2011; Nikolaeva *et al.*, 2013, 2014, 2015; Yermolaev *et al.*, 2010, 2014, 2015]. In particular, it was shown

that coefficients CE (and CE^*) of linear relation between Dst (and Dst^*) index and integral of interplanetary electric field $Ey = VxBz$ [Nikolaeva et al., 2013, 2015] depend on type of solar wind stream and at the same integral of Ey Sheath and CIR generate ~ 1.5 stronger magnetic storms than MC and Ejecta (see Table 1).

In discussed papers [Nikolaeva et al., 2013, 2015] a modification of function by Burton et al. [1975] connected Dst and Dst^* indices and interplanetary electric field Ey was used. Other FCs mentioned above have not been used for analysis of development of magnetic storms induced by various SW streams and for comparison of efficiencies of storm generation by these SW drivers. The aim of this brief paper is to check the dependence of efficiency of magnetic storm generation on type of solar wind stream using other coupling functions.

2. Data and methods

For analysis we use SW and IMF parameters of OMNI dataset (<http://omniweb.gsfc.nasa.gov>) [King and Papitashvili, 2004] and Kyoto dataset of Dst index measurements (<http://wdc.kugi.kyoto-u.ac.jp/index.html>). On the basis of these data we prepared the Catalog of large-scale interplanetary events for period of 1976–2000 and we select main phases of magnetic storms ($Dst_{min} \leq -50$ nT), generated by MC (10 storms, 77 1-h points), Ejecta (31 storms, 324 1-h points), Sheath (21 storms, 166 1-h points), CIR (31 storms, 279 1-h points) [Yermolaev et al., 2009; Nikolaeva et al., 2013, 2014, 2015].

The full set of 12 coupling functions is presented in the first column of the Table 2. They include 8 coupling functions (with our numbers FC1 – FC7, FC9) that were taken from paper [Borovsky and Birn, 2014], and 4 coupling functions (FC8, FC10, FC11, FC12) were suggested by other authors:

The function $FC1 = \sin^2(\theta/2)$ is the pure geometrical one; here clock angle θ is the IMF polar angle projected on $(Y - Z)_{GSM}$ plane (for example, [Sonnerup, 1974; Newell et al., 2007; Wilder et al., 2011; Borovsky and Birn, 2014]). Three coupling functions $FC2 = vByz$, $FC3 = vBz$, $FC4 = vBs$ are the different variants of electric field presentation by transverse component of IMF $Byz = (By^2 + Bz^2)^{1/2}$, by Bz component of IMF, and by Bs southward component of IMF [Burton et al., 1975; Hardy et al., 1981; Holzer et al., 1982]. Two coupling functions $FC5 = vByz \sin^2(\theta/2)$ and $FC6 = vByz \sin^4(\theta/2)$ are the electric field presentations with including clock angle dependence [Kan and Lee, 1979; Wygant et al., 1983]. The coupling function $FC7 = v^{4/3}Byz^{2/3} \sin^{8/3}(\theta/2)$ is the rate magnetic flux opened at the magnetopause [Newell et al., 2007]. It has the best correlation with nine from ten indices (with exception of Dst index) and present a nearly universal SW–Magnetosphere coupling function obtained from ten magnetospheric state variables [Newell et al., 2007]. The coupling function $FC9 = Rquick$ is the reconnection rate on the dayside of the magnetosphere obtained with methodology of Borovsky (see, paper [Borovsky and Birn, 2014] and references inside). $Rquick \sim \sin^2(\theta/2)C^{-1/2}n^{1/2}v^2(1 + \beta_s)^{-3/4}$, where β_s is the plasma beta of magnetosheath, C is the compression ratio of the bow shock. Both β_s and C are functions of the Alfvén Mach number M_A (see, expressions (3)–(8) in paper [Borovsky and Birn, 2014]). $FC8 = p^{1/2}v^{4/3}Byz^{2/3} \sin^{8/3}(\theta/2)$ is the best coupling function for Dst index prediction which differs from nearly universal $FC7$ inferred from 10 magnetospheric state variables by dynamic pressure factor $p^{1/2}$ (correction on the magnetopause currents) [Newell et al., 2007]. $FC10 = p^{1/2}v^{4/3}Byz \sin^6(\theta/2)$ is the best function for Dst index prediction in non-linear dynamic systems [Temerin and Li, 2006; Balikhin et al., 2010] and includes the correction on dynamic pressure and the IMF clock-

angle θ dependence as $\sin^6(\theta/2)$; it was followed from model by *Kan and Lee* [1979] when dependence of reconnection line length on clock angle θ was included [*Balikhin et al.*, 2010]. $FC11 = V_{sw} + 56Bs$ is the function without any clear physical interpretation, or mathematical variant with the best correlation [*Borovsky*, 2014]. $FC12 = M_A$ is the Alfvén Mach number (the ratio of SW velocity to Alfvén speed). The dependence on M_A is included in function $FC9 = R_{quick}$ (see, [*Borovsky and Birn*, 2014]), but $FC12$ allows one to analyse only dependence on M_A .

To compare the interplanetary drivers we estimate an efficiency of magnetic storm generation by type of solar wind stream with using 12 coupling functions. For each type of the SW stream the coefficients, C_{FCN} and C_{FCN}^* were obtained by the linear approximation of Dst and Dst^* indices: $Dst_i = C_0 + C_{FCN}FCN_i$, $Dst_i^* = C_0^* + C_{FCN}^*FCN_i$ where i is the point number at the main phase of magnetic storms induced by given type of SW stream, and FCN are coupling functions $FC1 - FC12$. Obtained approximation coefficients C_{FCN} and C_{FCN}^* are interpreted as efficiencies of Dst and Dst^* generation and presented in Table 3. The correlation coefficients for these fits which are connected with the accuracy of the description of SW-magnetosphere connections for corresponding coupling function, change in rather wide interval - from 0.01 up to 0.63 (see Figure 1). As mentioned above, the statistics of points for approximation is rather high - from 77 points for MC up to 329 for Ejecta (see, Table 3). So, in most cases of calculated coefficients C_{FCN} and C_{FCN}^* are obtained with good statistical significances. Reliability of coefficients C_{FCN} and C_{FCN}^* are connected with many parameters (data series, statistics, type of coupling function etc.) and requires further investigations which will be made in our future works. To obtain a rough estimation of a total (on all 12 coupling functions) characteristics of efficiency of

magnetic storm generation by different types of solar wind stream, the absolute values of approximation coefficients for each coupling function were ranked on types of the solar wind stream, i.e. values from 1 (for the lowest coefficient) to 4 (for the highest coefficient) were appropriated to the corresponding efficiencies (see numbers in parentheses). Last line of Table 3 presents the average values of efficiency defined by this method which maybe called "place number" method. Because the average value of sequence 1, 2, 3, and 4 is 2.5 $((1+2+3+4)/4=2.5)$, the average values over $12FCs > 2.5$ means that for given SW type the most part of FCs have high efficiencies.

3. Results

Table 2 presents the average values (signed by $\langle \rangle$), standard deviations and medians of values of twelve coupling functions FC1 – FC12 calculated at the main phase of magnetic storms induced by 4 types of SW drivers. These data show that all FCs have large deviations of values and average values can depend on SW type. Behaviour of FCs at the main phase of storms is determined by changes of corresponding SW and IMF parameters (see, for instance, average dynamics of parameters for CIR, Sheath, MC and Ejecta in papers by *Yermolaev et al.* [2010, 2015]).

The Table 3 data allow one to estimate the efficiency of the magnetic storm generation by the different SW types. The lowest negative coefficients values C_{FCN} and C_{FCN}^* (or the highest values of their magnitude) indicate the highest efficiencies of SW type for given coupling function FCN, because at the equal values of FCN the calculated value of Dst (or Dst^*) is lower (magnetic storm is stronger). In the contrast with the most values of C_{FCN} and C_{FCN}^* magnitude, the lowest values of them indicate the lower values

of efficiencies. Table 3 shows that for each coupling function the different SW types can be the most effective for development of main phase of magnetic storm.

For description of Dst at the main phase of Sheath-driven storms the most efficiency is associated with five FCs (FC4, FC6, FC7, FC9, FC11); for CIR-driven storms - two FCs (FC2, FC8); for the MC-driven storms - two FCs (FC3, FC12), and for Ejecta-driven storms - three FCs (FC1, FC5, FC10). Similarly for corrected (on dynamic pressure) Dst^* at the main phase of Sheath-driven storms the most efficiency is related with seven FCs (FC3, FC4, FC5, FC6, FC7, FC9, FC11); for CIR-driven storms - only FC2; for MC-driven storms - only FC12, for Ejecta-driven storms - two FCs (FC1, FC8). In particular, we can see in Table 3 that the coefficients of linear relation between Dst (and Dst^*) indices and coupling function $F9 = Rquick$ depend on type of solar wind stream, and Sheath and CIR generate ~ 1.42 and ~ 1.38 stronger magnetic storms than MC in agreement with data presented in Table 1 [Nikolaeva et al., 2013, 2015].

Because of different dimensionality of C_{FCN} and C_{FCN}^* , their different ranges of changes, different distributions and so on, it is impossible to directly compare them for different FCs. To overcome these difficulties we use method of "place number" described in the Data and Method Section. This method allows us to obtain that in average Sheath have more large efficiency of the magnetic storm generation and MC have more low efficiency (in factors ~ 1.4 and ~ 1.7 for Dst and Dst^* , respectively) in agreement with our previous results.

4. Discussion

The carried-out analysis allowed us to obtain rather unexpected results. On the one hand, the found distinctions in efficiency of storm generation with various drivers allow

to answer the question raised in the article title positively: Yes, generation of magnetic storms depends on the type of solar wind. On the other hand, ratios of efficiencies of various SW types differ for various functions (or physical models) connecting parameters of the interplanetary space and calculated (modeled) values of Dst and Dst^* indices. The answer to a question "Why it so happens?" is beyond the scope work. Here we will discuss only the general approaches to the solution of this problem.

It should be noted that the dependence of efficiency of magnetic storm generation by different SW types on type of coupling function can be associated with following causes:

1. An accuracy of physical process description. Different coupling functions (or used physical models) have different accuracy of geomagnetic index prediction on the basis of measured interplanetary plasma and IMF parameters.
2. Used data set. Obtained results are related with specific data selection. The stability of obtained results with other data sets requires further study.
3. An accuracy of data approximation. Although the approximation accuracy is directly related with two previous problems, its analysis could provide additional information for a more reliable conclusion about the differences between efficiency of magnetic storms generation by different SW types.

The correlation coefficients are one of the criterion of the accuracy of data approximation and correlation coefficients between measured Dst and pressure corrected Dst^* indices and 12 coupling functions during main phases of magnetic storms driven by different solar wind streams are presented in Figure 1. The most part of correlation coefficients has sufficiently high values. In particular the highest values of coefficients (~ 0.5 up to ~ 0.63) are observed for Sheath- driven storms. So, conclusion about high efficiency of

Sheath is reliable. In a small part of low coefficients it is necessary to increase the number of magnetic storms to increase the statistical significance of results. Nevertheless, we believe that obtained results can be considered as a basis for further investigation.

5. Conclusions

Thus on the OMNI data for interval 1976–2000 we study the generation of magnetic storms induced by MC (10 storms, 77 points), Sheath (21 storms, 166 points), Ejecta (31 storms, 324 points), CIR (31 storms, 279 points) and evaluate the dependence of efficiency of magnetic storm generation on type of SW stream using 12 coupling functions. Also we estimated the correlation coefficients between 12 coupling functions and measured Dst and pressure corrected Dst^* indices during the main phases of magnetic storms.

Our study allowed to obtain the following results

1) The generation of magnetic storm depends on type of solar wind in agreement with previous results [*Borovsky and Denton, 2006; Huttunen et al., 2006; Pulkkinen et al., 2007; Yermolaev et al., 2007; Plotnikov and Barkova, 2007; Longden et al., 2008; Turner et al., 2009; Guo et al., 2011; Nikolaeva et al., 2013, 2014, 2015; Yermolaev et al., 2010, 2014, 2015*].

2) The most part of the coupling functions have the high efficiency for Sheath in agreement with our result presented in previous papers [*Nikolaeva et al., 2013, 2015*].

3) In contrast with Sheath the most part of coupling functions for MC have the lowest efficiencies. This also confirm our results [*Nikolaeva et al., 2013, 2015*].

4) Efficiencies of magnetic storm generation by CIR and Ejecta are intermediate.

We consider that the results presented here are preliminary: the confirmation of these results, increase in their reliability require further investigation, and we plan to continue this analysis.

Acknowledgments. The authors are grateful for the opportunity to use the OMNI database. The OMNI data were obtained from GSFC/ SPDF OMNIWeb (<http://omniweb.gsfc.nasa.gov>). This work was supported by the Russian Foundation for Basic Research, projects 13–02–00158 and 16–02–00125, and by Program of Presidium of the Russian Academy of Sciences.

References

- Balikhin, M. A., R. J. Boynton, S. A. Billings, M. Gedalin, N. Ganushkina, D. Coca, and H. Wei (2010), Data based quest for solar wind-magnetosphere coupling function, *Geophys. Res. Lett.*, 37, L24107, doi:10.1029/2010GL045733.
- Borovsky, J. E. and Denton, M.H. (2006), Differences between CME-Driven Storms and CIR-Driven Storms, *J. Geophys. Res.*, 28, 121–190.
- Borovsky, J. E. (2008), The rudiments of a theory of solar-wind/magnetosphere coupling derived from first principles, *J. Geophys. Res.*, 113, A08228, doi:10.1029/2007JA012646.
- Borovsky, J. E. (2013a), Physical improvements to the solar-wind reconnection control function for the Earths magnetosphere, *J. Geophys. Res. Space Physics*, 118, 2113–2121, doi:10.1002/jgra.50110.
- Borovsky, J. E. (2013b), Physics based solar-wind driver functions for the magnetosphere: Combining the reconnection-coupled MHD generator with the viscous interaction, *J. Geophys. Res. Space Physics*, 118, 7119–7150, doi:10.1002/jgra.50557.

- Borovsky, J. E., and J. Birn (2014), The solar wind electric field does not control the day-side reconnection rate, *J. Geophys. Res. Space Physics*, 119, doi:10.1002/2013JA019193.
- Borovsky J. E. (2014), Canonical correlation analysis of the combined solar-wind and geomagnetic-index data sets , *JGR*, doi: 10.1002/2013JA019607
- Burton, R. K., McPherron, R. L., and Russell, C. T (1975), An empirical relationship between interplanetary conditions and Dst, *J. Geophys. Res.*, 80, 4204–4214.
- Cassak, P. A., and M. A. Shay (2007), Scaling of asymmetric magnetic reconnection: General theory and collisional simulations, *Phys. Plasmas*, 14, 102, 114.
- Guo, J., X. Feng, B. A. Emery, J. Zhang, C. Xiang, F. Shen, and W. Song (2011), Energy transfer during intense geomagnetic storms driven by interplanetary coronal mass ejections and their sheath regions, *J. Geophys. Res.*, 116, A05106, doi:10.1029/2011JA016490
- Hardy, D. A., W. J. Burke, M. S. Gussenhoven, N. Heinemann, and E. Holeman (1981), DMSP/F2 electron observations of equatorward auroral boundaries and their relationship to the solar wind velocity and north-south component of the interplanetary magnetic field, *J. Geophys. Res.*, 86, 9961.
- Holzer, R. E. and J. A. Slavin (1982), An evaluation of three predictors of geomagnetic activity, *J. Geophys. Res.*, 87(A4), 2558–2562.
- Huttunen, K.E.J., Koskinen, H.E.J., Karinen, A., and K. Mursula (2006), Asymmetric development of magnetospheric storms during magnetic clouds and sheath regions, *Geophys. Res. Lett.*, 33, L06107, doi: 10.1029/2005GL024894.
- Kan, J. R., and L. C. Lee (1979), Energy coupling function and solar wind-magnetosphere dynamo, *Geophys. Res. Lett.*, 6, 577–580.

- King, J.H. and N.E.Papitashvili (2004), Solar Wind Spatial Scales in and Comparisons of Hourly Wind and ACE Plasma and Magnetic Field Data, *J. Geophys. Res.*, 110, A2, A02209, doi: 10.1029/2004JA010804.
- Longden, N., M. H. Denton, and F. Honary (2008), Particle precipitation during ICME-driven and CIR-driven geomagnetic storms, *J. Geophys. Res.*, 113, A06205, doi:10.1029/2007JA012752.
- Newell, P. T., T. Sotirelis, K. Liou, C.-I. Meng, and F. J. Rich (2007), A nearly universal solar wind-magnetosphere coupling function inferred from 10 magnetospheric state variables, *J. Geophys. Res.*, 112, A01206, doi:10.1029/2006JA012015.
- Nikolaeva, N. S., Y. I. Yermolaev, and I. G. Lodkina (2013), Modeling of Dst-index temporal profile on the main phase of the magnetic storms generated by different types of solar wind, *Cosmic Res.*, 51 (6), 401–412. (*Kosmicheskie Issledovaniya*, 2013, vol. 51, N 6, pp. 443–454).
- Nikolaeva N. S., Yu. I. Yermolaev, and I. G. Lodkina (2014), Dependence of Geomagnetic Activity during Magnetic Storms on Solar Wind Parameters for Different Types of Streams: 4. Simulation for Magnetic Clouds, *Geomagnetism and Aeronomy*, Vol. 54, No. 2, pp. 152–161.
- Nikolaeva, N. S., Y. I. Yermolaev, and I. G. Lodkina (2015), Modeling of the corrected Dst* index temporal profile on the main phase of the magnetic storms generated by different types of solar wind, *Cosmic Res.*, 53(2), 119–127.
- Plotnikov, I. Y., and E. S. Barkova (2007), Nonlinear dependence of Dst and AE indices on the electric field of magnetic clouds, *Adv. Space Res.*, 40, 1858–1862.

- Pulkkinen, T. I., Partamies, N., Huttunen, K. E. J., Reeves, G. D., and H. E. J. Koskinen (2007), Differences in geomagnetic storms driven by magnetic clouds and ICME sheath regions, *Geophys. Res. Lett.*, 34, L02105, doi:10.1029/2006GL027775.
- Sonnerup B. U. O. (1974), Magnetopause Reconnection Rate, *J. Geophys. Res.*, 79, 10, 1546–1549.
- Temerin, M., and X. Li (2006), Dst model for 19952002, *J. Geophys. Res.*, 111, A04221, doi:10.1029/2005JA011257.
- Turner, N. E., W. D. Cramer, S. K. Earles, and B. A. Emery (2009), Geoefficiency and energy partitioning in CIR-driven and CME-driven storms, *J. Atmos. Sol. Terr. Phys.*, 71, 1023–1031.
- Wilder, F. D., C. R. Clauer, J. B. H. Baker, E. P. Cousins, and M. R. Hairston (2011), The nonlinear response of the polar cap potential under southward IMF: A statistical view, *J. Geophys. Res.*, 116, A12229, doi:10.1029/2011JA016924.
- Wygant, J. R., R. B. Torbert, and F. S. Mozer (1983), Comparison of S3-3 polar cap potential drops with the interplanetary magnetic field and models of magnetopause reconnection, *J. Geophys. Res.*, 88, 57275735.
- Yermolaev, Yu. I., Yermolaev, M. Yu., Nikolaeva, N. S., and L. G. Lodkina (2007), Interplanetary conditions for CIR-induced and MC induced geomagnetic storms, *Bulg. J. Phys.*, 34, 128–135.
- Yermolaev, Yu.I., Nikolaeva, N.S., Lodkina, I.G., and M.Yu. Yermolaev (2009), Catalog of large-scale solar wind phenomena during 1976–2000, *Cosmic Research*, vol. 47, no. 2, pp. 81–94.

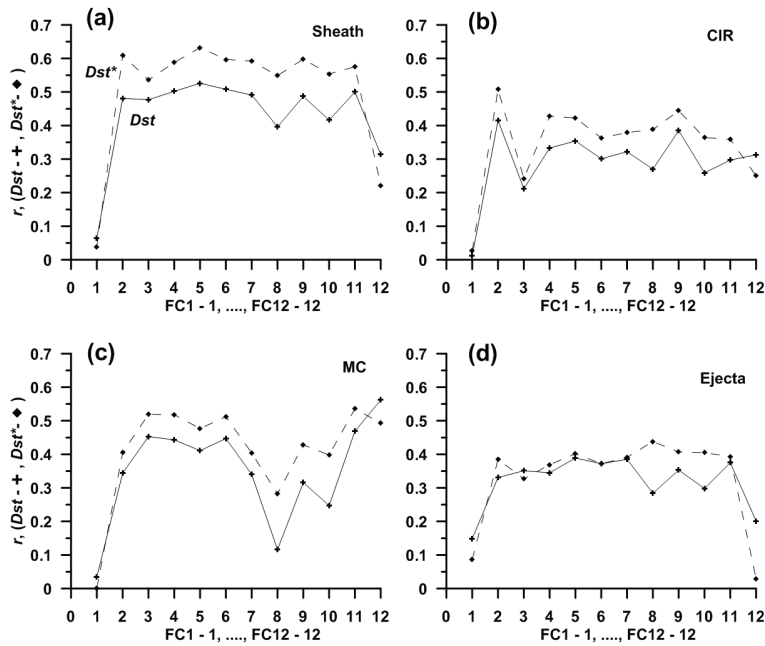


Figure 1. Correlation coefficients, r , between measured Dst (crosses, and solid line) and pressure corrected Dst^* (diamonds, and dotted line) indices and the values of 12 coupling functions FC1–FC12 during the main phases of magnetic storms driven by: (a) Sheath; (b) CIR; (c) MC; (d) Ejecta

Yermolaev, Y. I., N. S. Nikolaeva, I. G. Lodkina, and M. Y. Yermolaev (2010), Specific interplanetary conditions for CIR-induced, Sheath-induced, and ICME-induced geomagnetic storms obtained by double superposed epoch analysis, *Ann. Geophys.*, 28, 21772186.

Yermolaev, Y. I., I. G. Lodkina, N. S. Nikolaeva, and M. Y. Yermolaev (2014), Influence of the interplanetary driver type on the durations of the main and recovery phases of magnetic storms, *J. Geophys. Res.*, 119, 10, 8126–8136, doi:10.1002/2014JA019826.

Yermolaev, Yu. I., I. G. Lodkina, N. S. Nikolaeva, and M. Yu. Yermolaev (2015), Dynamics of large-scale solar wind streams obtained by the double superposed epoch analysis, *J. Geophys. Res.*, 120, doi:10.1002/2015JA021274.

Table 1. The coefficients CE (and CE^*) of linear relation between Dst and Dst^* indices and integral of interplanetary electric field $Ey = VxBz$ at the main phases of magnetic storms driven by different solar wind streams [Nikolaeva et al., 2013, 2015].

SW type	MC	Ejecta	Sheath	CIR
CE (for Dst)	2.55 ± 0.75	2.3 ± 1.0	3.2 ± 1.6	2.8 ± 1.1
CE^* (for Dst^*)	2.0 ± 1.1	2.1 ± 1.1	3.4 ± 1.9	3.0 ± 1.5

Table 2. The average values of 12 coupling functions with standard deviation and median values at the main phases of magnetic storms driven by MC, Ejecta, Sheath, CIR.

FC type	MC-storms		Ejecta-storms		Sheath-storms		CIR-storms	
	$\langle \rangle$	median	$\langle \rangle$	median	$\langle \rangle$	median	$\langle \rangle$	median
FC1= $\sin^2(\theta/2)$	0.91 ± 0.11	0.93	0.84 ± 0.19	0.92	0.82 ± 0.19	0.87	0.795 ± 0.22	0.88
FC2= $vByz$	4.61 ± 2.39	3.86	3.83 ± 1.49	3.69	5.66 ± 3.86	4.40	4.29 ± 1.97	3.91
FC3= vBz	3.69 ± 1.87	3.26	2.60 ± 1.80	2.60	3.50 ± 3.36	3.05	2.56 ± 2.36	2.62
FC4= vBs	3.74 ± 1.82	3.23	2.87 ± 1.48	2.66	3.93 ± 2.9	3.28	3.16 ± 1.87	2.81
FC5= $vByz \sin^2(\theta/2)$	4.15 ± 2.04	3.44	3.21 ± 1.45	3.06	4.58 ± 3.29	3.59	3.42 ± 1.87	3.05
FC6= $vByz \sin^4(\theta/2)$	3.78 ± 1.87	3.26	2.83 ± 1.49	2.65	3.91 ± 3.03	3.19	2.94 ± 1.91	2.64
FC7= $v^{4/3}Byz^{2/3} \sin^{8/3}(\theta/2)$	13.83 ± 5.30	12.35	11.70 ± 4.95	11.04	14.86 ± 9.35	12.81	11.49 ± 5.61	10.92
FC8= $p^{1/2}v^{4/3}Byz^{2/3} \sin^{8/3}(\theta/2)$	25.02 ± 12.09	21.36	23.69 ± 13.74	21.28	37.01 ± 40.68	23.91	26.6 ± 16.3	21.83
FC9= <i>Rquick</i>	172.43 ± 69.76	149	147.4 ± 58.4	136	194.83 ± 122.94	158	159.4 ± 79.35	142.36
FC10= $p^{1/2}v^{4/3}Byz \sin^6(\theta/2)$	47.74 ± 28.34	38.89	40.41 ± 30.85	32.69	68.52 ± 84.51	40.30	46.92 ± 40.52	32.84
FC11= $Vsw + 56Bs$	910.3 ± 231.2	850	792.7 ± 198.01	780	904.1 ± 349.2	850	801.5 ± 251.34	769
FC12= M_A	6.90 ± 3.36	6.3	8.45 ± 3.38	7.7	7.42 ± 3.59	6.5	8.70 ± 3.85	7.66

Table 3. Coefficients of the linear relation between the Dst and Dst^* indices and the coupling function values at the main phase of magnetic storms driven by 4 types of the SW.

FC type	MC, 77 points		Ejecta, 324 points		Sheath, 166 points		CIR, 279 points	
	C_{FCN}	C_{FCN}^*	C_{FCN}	C_{FCN}^*	C_{FCN}	C_{FCN}^*	C_{FCN}	C_{FCN}^*
FC1	-8.01 (2)	0.26 (1)	-20.6 (4)	-12.8 (4)	-14.4 (3)	-9.11 (3)	-1.79 (1)	4.58 (2)
FC2	-3.77 (1)	-4.41 (1)	-5.88 (3)	-7.35 (2)	-5.35 (2)	-7.38 (3)	-7.16 (4)	-9.20 (4)
FC3	-6.35 (4)	-7.23 (3)	-5.19 (2)	-5.18 (2)	-6.09 (3)	-7.44 (4)	-3.03 (1)	-3.75 (1)
FC4	-6.37 (4)	-7.42 (2)	-6.23 (2)	-7.18 (1)	-7.20 (4)	-9.25 (4)	-5.81 (1)	-8.05 (3)
FC5	-5.29 (1)	-6.10 (1)	-7.13 (4)	-7.91 (2)	-6.86 (3)	-8.96 (4)	-6.42 (2)	-8.19 (3)
FC6	-6.26 (2)	-7.14 (3)	-6.65 (3)	-7.13 (2)	-7.17 (4)	-9.16 (4)	-5.36 (1)	-6.92 (1)
FC7	-1.68 (1)	-1.99 (1)	-2.06 (3)	-2.25 (2)	-2.25 (4)	-2.95 (4)	-1.95 (2)	-2.46 (3)
FC8	-0.25 (1)	-0.61 (1)	-0.55 (3)	-0.91 (4)	-0.42 (2)	-0.63 (2)	-0.56 (4)	-0.85 (3)
FC9	-0.12 (1)	-0.16 (1)	-0.16 (2)	-0.20 (2)	-0.17 (4)	-0.23 (4)	-0.16 (3)	-0.20 (3)
FC10	-0.23 (3)	-0.36 (3)	-0.26 (4)	-0.37 (4)	-0.21 (1)	-0.31 (1)	-0.22 (2)	-0.32 (2)
FC11	-0.05 (3)	-0.06 (3)	-0.05 (2)	-0.06 (2)	-0.06 (4)	-0.08 (4)	-0.04 (1)	-0.05 (1)
FC12	4.38 (4)	3.86 (4)	1.59 (1)	0.25 (1)	3.75 (3)	2.86 (3)	2.76 (2)	2.28 (2)
rel. aver	2.17	2.00	2.75	2.33	3.08	3.33	2.00	2.33